Remanent moment of high-temperature superconductors: Implications for flux-pinning and glassy models

A. P. Malozemoff, L. Krusin-Elbaum, D. C. Cronemeyer, Y. Yeshurun,* and F. Holtzberg
IBM Thomas J. Watson Research Center, Yorktown Heights, New York 10598-0218
(Received 5 May 1988)

Superconducting quantum interference device (SQUID) magnetometer data on a variety of ceramics and crystals of Y-Ba-Cu-O show a remanent moment which accurately equals the difference of the field-cooled and zero-field-cooled moments in the low-field, low-temperature range. This effect is argued to point to a flux pinning rather than a superconductive glass model, particularly for the crystals. This holds true even when the glassy model is extended to include screening effects.

I. INTRODUCTION

Complementing preliminary reports,[1-5] we present here more complete data on the low-temperature remanent moment as well as the related Meissner fraction (field-cooled moment) of ceramic and crystal Y-Ba-Cu-O over a field range from 10 mOe (1 μT) to 60 Oe (6 mT). We also extend the earlier discussion[3] of the remanent moment in both flux pinning and superconductive glass models.

Measurements of the Meissner fraction, that is, of the field-cooled moment normalized by internal field, have been widely used to estimate the fraction of superconducting material, particularly in studies of the new high-temperature superconductors. The data we show here and have shown earlier[1-5] demonstrate this to be unreliable since the fraction depends strongly on the field applied during the experiment. We have earlier proposed a theory of this effect[5] based on flux line pinning; we will treat this aspect of the problem in greater detail elsewhere.

Here we focus on the low-temperature remanent moment $M_{\rm rem}$, which is consistently equal to the difference between the field-cooled (FC) and zero-field-cooled (ZFC) moments $M_{\rm FC}-M_{\rm ZFC}$ in the same low-field range where the Meissner fraction is changing strongly with field. This simple rule is important because it sheds light on the interpretation of magnetic properties in these superconductors. Two rather different models have been proposed, one drawing on conventional flux-pinning concepts[6-8] in type-II superconductivity, the other based on the notion of a granular superconductive glass.[9-11] We argue that random polarity reversal of local moments is a unique and defining characteristic of the superconducting glass state and is revealed experimentally by the difference between $M_{\rm rem}$ and $M_{\rm FC}-M_{\rm ZFC}$. Thus the equality of $M_{\rm rem}$ and $M_{\rm FC}-M_{\rm ZFC}$ indicates that superconductive glass effects make a negligibly small contribution to the macroscopic magnetic properties of these superconductors at least in the low-field low-temperature range. These concepts should apply also to conventional low-temperature superconductors.

II. EXPERIMENTAL RESULTS

As described earlier,[3-5] the measurements were performed on a noncommercial SQUID magnetometer with μ-metal shielding and a solenoid electromagnet which permits measurements in fields ranging from a few mOe to about 60 Oe, depending on the size of the signal. The background field is generally $\sim\frac{1}{2}$ mOe. The sample is moved between counterwound pickup coils connected to a SHE SQUID probe. The sample is suspended on a phenolic holder in an exchange gas chamber of high-purity copper, which is resistively heated to control temperature. The very small fields and sample sizes in certain cases give small signals; so special precautions must be taken to avoid or correct for spurious background signals, as described in the Appendix.

The samples are first cooled to low temperature in the background field ("zero field"). The field is subsequently applied and moment measured as a function of slowly increasing temperature, yielding curves labeled ZFC (zero-field cooled) in Figs. 1–6. The temperature is then slowly reduced through the superconducting transition, yielding the curves labeled FC (field cooled) in the figures. Finally, the field is turned off at low temperature (from 4 to 20 K; usually the measured moments are essentially temperature independent below 20 K or so). The resulting moment was measured as a function of slowly increasing temperature, yielding curves labeled REM (remanent) in the figures.

The data represent slow runs (half a day for one temperature run from T_c on down or vice versa), with the hope of approaching equilibrium as closely as possible. However, both the ZFC and REM data are intrinsically metastable, and even the FC data may have some time effects, particularly in the high-temperature regime.[12,13] Only at low temperatures are all these data independent of time to within experimental accuracy. Most earlier studies of time effects have usually been conducted at higher applied fields.[14-16]

Figures 1 and 2 exhibit the full temperature runs for an Y-Ba-Cu-O single crystal (sample *c* in Table I). Similar

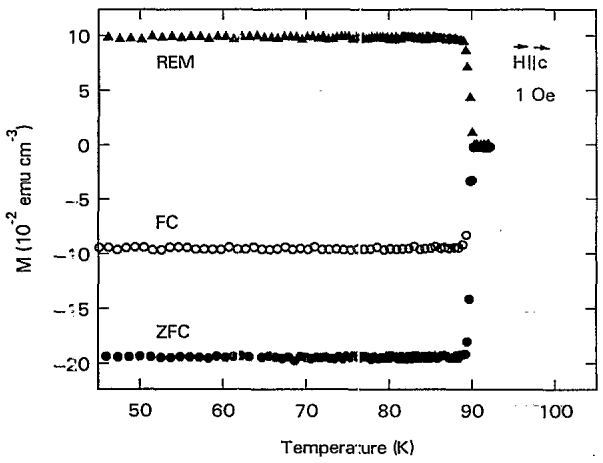

FIG. 1. Zero-field-cooled (ZFC), field-cooled (FC), and remanent (REM) moments as a function of temperature, for a 0.25-mg Y-Ba-Cu-O crystal (Ref. 19) (see Table I) with a 1-Oe field applied parallel to the c axis.

curves are obtained for conventional superconductors such as V_3Si, and, in particular, the low-temperature value of the remanent magnetization equals the difference between the FC and the ZFC values in all cases, at least in the low-field regime we are considering here. We exhibit here data for Y-Ba-Cu-O only. A comparative study of high-temperature and conventional superconductors will be presented elsewhere.

These data are generally temperature independent through most of the region well below T_c, except for the ultrathin Y-Ba-Cu-O crystal (sample d of Table I) which shows slight temperature dependence even at low temperatures. Some interesting anomalies occur in the high-temperature region around T_c, but in this paper we concentrate on the low-temperature data. Figures 3–6 show the field dependence of the low-temperature zero-field-cooled (ZFC), field-cooled (FC), and remanent (REM) moments of a set of different superconducting samples (b–d in Table I). Data on sample a have been given in Ref. 3. The data are normalized by applied field but uncorrected for demagnetization effects, for reasons to be described below. The remanent moment, observed in zero applied field, is normalized by the applied field during the preceding field cooling.

The figures also show the difference between FC and

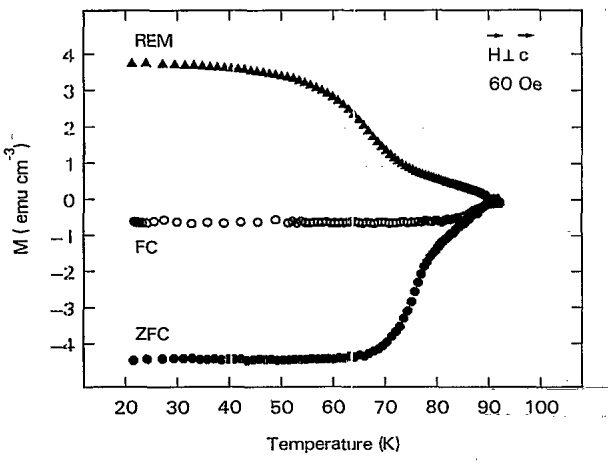

FIG. 2. Zero-field-cooled (ZFC), field-cooled (FC), and remanent (REM) moments as a function of temperature, for a 0.25-mg Y-Ba-Cu-O crystal (Ref. 19) (see Table I) with 60-Oe field applied perpendicular to the c axis. There is a noteworthy broadening of the transition as compared to the 1-Oe data in Fig. 6.

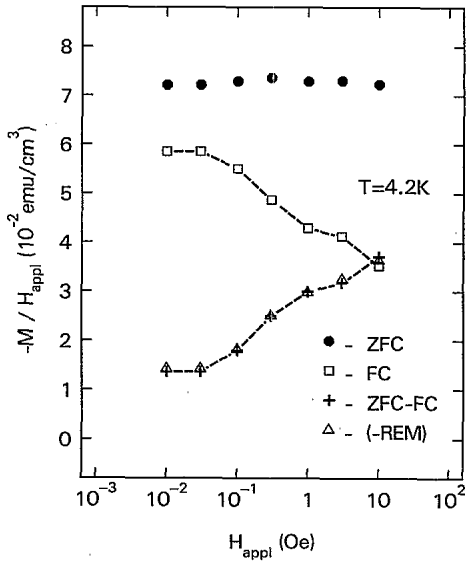

FIG. 3. Low-temperature zero-field-cooled (ZFC), field-cooled (FC), and remanent (REM) moments, normalized by applied field H_{appl}, for a high-density Y-Ba-Cu-O ceramic (Ref. 18) (see Table I). The difference of M_{FC} and M_{ZFC} is compared to M_{rem}; they are closely equal.

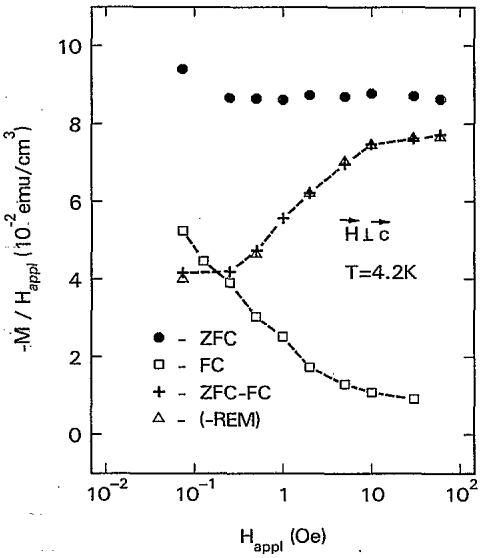

FIG. 4. Low-temperature zero-field-cooled (ZFC), field-cooled (FC), and remanent (REM) moments, normalized by applied field H_{appl}, for a 0.25-mg Y-Ba-Cu-O crystal (Ref. 19) (see Table I) with field applied perpendicular to the c axis. The difference of M_{FC} and M_{ZFC} is compared to M_{rem}; they are closely equal.

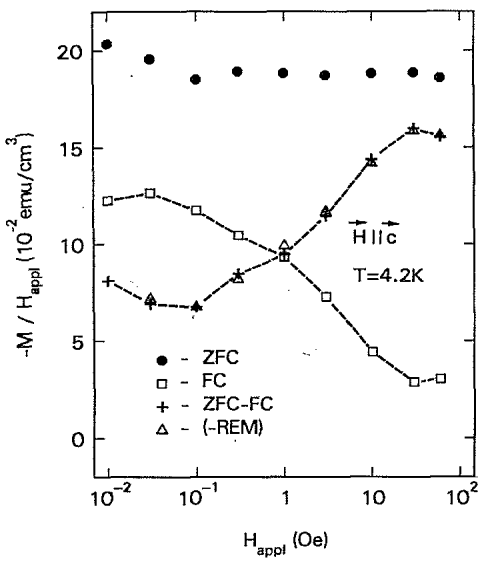

FIG. 5. Low-temperature zero-field-cooled (ZFC), field-cooled (FC), and remanent (REM) moments, normalized by applied field H_{appl}, for a 0.25-mg Y-Ba-Cu-O crystal (Ref. 19) (see Table I) with field applied parallel to the c axis. The difference of M_{FC} and M_{ZFC} is compared to M_{rem}; they are closely equal.

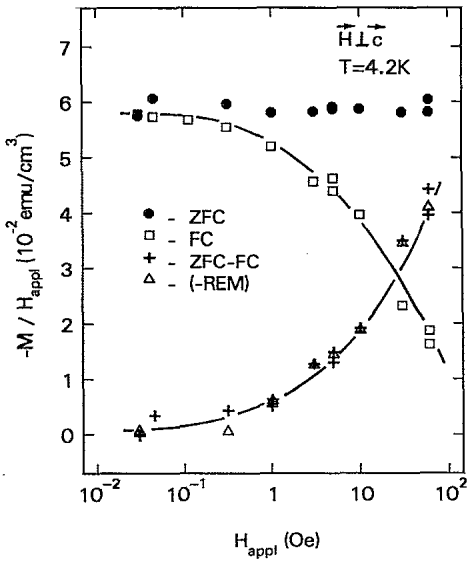

FIG. 6. Low-temperature zero-field-cooled (ZFC), field-cooled (FC), and remanent (REM) moments, normalized by applied field H_{appl}, for a 0.13-mg, 20-μm-thick Y-Ba-Cu-O crystal (Ref. 19) (see Table I) with field applied perpendicular to the c axis. The difference of M_{FC} and M_{ZFC} is compared to M_{rem}; they are closely equal. Note the shift to higher fields of the dropoff in M_{FC}.

ZFC moments, normalized to applied field, compared to the remanent moment normalized by the same applied field as described above. The two sets of data are essentially equal within experimental error for all samples and fields. The significance of this simple rule will be discussed below.

Properties and characteristics of the different Y-Ba-Cu-O samples are described in Table I.[17–19] A ceramic $La_{1.8}Sr_{0.2}CuO_4$ sample was studied earlier in Ref. 1, and a low-density Y-Ba-Cu-O ceramic[17] in Ref. 3. The only weakly field-dependent Meissner fraction of that low-density ceramic contrasts with the much stronger field dependence shown in Fig. 3 for the high-density ceramic. The crystals also show a strong effect for field in both principal orientations, as shown in Figs. 4 and 5. Since the demagnetizing factors for these two orientations are quite different (see Table I), it is clear that this field dependence is not some artifact of demagnetization but is a bulk material property, whose origin has been described elsewhere.[5] Similar results have been obtained for a different Y-Ba-Cu-O crystal prepared by a different growth technique and reported on in Ref. 4. Finally, in Fig. 6 data on a much thinner Y-Ba-Cu-O crystal are shown. The dropoff in the Meissner fraction is shifted to higher fields. Optical microscopy indicates a comparable twin density in the crystal, but the reason for the difference in the Meissner effect requires further investigation. Further discussion of these effects will be presented elsewhere; in what follows we focus on the remanent moment and its simple relation to the field-cooled and zero-field-cooled moments in all these samples.

III. DISCUSSION: REMANENT MOMENT IN THE FLUX-PINNING MODEL

We discuss next how the remarkable agreement between the remanent moment and the difference between the field-cooled and zero-field-cooled moments can be understood in a flux-pinning model. In Sec. IV we show how this effect can be used to measure the importance of superconductive glass behavior in the macroscopic magnetic

TABLE. I. Properties of superconducting samples.

Sample	Description	Ref.	Weight (mg)	Approximate demagnetization factor	T_c
a	Y-Ba-Cu-O, ceramic, low density	17	42	0.031	90.2
b	Y-Ba-Cu-O, ceramic, 95% density	18	4.0	0.10	89
c	Y-Ba-Cu-O, crystal, H∥c	19	0.25	0.63	90.2
	H⊥c			0.16	
d	Y-Ba-Cu-O, 20-μm-thick crystal	19	0.13	0.01	90.4

properties.

The equality of $M_{\rm rem}$ and $M_{\rm FC}-M_{\rm ZFC}$ has a natural explanation in the standard picture of flux pinning in type-II superconductors.[6-8] Let us first neglect demagnetizing effects, to which we return later. B, the magnetic induction, is the spatial average over $h(x)$, the local induction field at position x in the sample, which is determined by the specific vortex structure of the superconductor. It is simply related to the applied field by $B=H_a+4\pi M$, as usual.

In the zero-field-cooled state at low fields with minimal flux penetration, $-4\pi M$ is determined by the difference between the applied field and $h(x)$, as shown schematically by the shaded region in Fig. 7(a). The falloff at the sample edges is due to London penetration, a negligibly small effect except in the thinnest samples. By contrast, in the field-cooled state, flux is trapped in the sample, as has been described elsewhere.[5] Once again $-4\pi M$ is the difference between the applied field and $h(x)$, as shown schematically by the shaded region in Fig. 7(b). Finally, turning off the field, $4\pi M$ becomes B, as shown in Fig. 7(c). The $h(x)$ contour cannot shift in the bulk of the sample because of the assumed pinning. Provided surface effects are negligible, the two shaded areas of Figs. 7(b) and 7(c) add up to that of Fig. 7(a). In other words [noting that in Figs. 7(a) and 7(b) the shaded areas represent negative M],

$$M_{\rm rem}=M_{\rm FC}-M_{\rm ZFC}. \tag{1}$$

In the presence of a finite demagnetizing factor N, a question arises of how to properly compare $M_{\rm rem}$ with $M_{\rm FC}-M_{\rm ZFC}$. Should one use, for example, magnetization corrected for demagnetizing factors or not? We show next that to test the flux-pinning model, one must simply compare the raw measured magnetizations corresponding to a given *applied* field. On the other hand, to test the theory of $M_{\rm FC}$ described earlier,[5] one must use the measured moment with the demagnetization-corrected internal field of the field-cooled measurement.

To explain these points it is first necessary to recognize that a magnetometer such as the SQUID system we use here measures the total dipole moment of the sample, irrespective of the demagnetizing fields, and the dipole moment is determined by M, the magnetization or moment per unit volume, times the sample volume. Next we use the classic relation for the magnetic induction

$$B=H_i+4\pi M, \tag{2}$$

where the internal field is

$$H_i=H_a-4\pi NM. \tag{3}$$

The measured zero-field-cooled moment, assuming complete exclusion of flux, is just $M_{\rm ZFC}=-H_i/4\pi$, which leads to

$$M_{\rm ZFC}=-H_a/4\pi(1-N). \tag{4}$$

The measured field-cooled moment $M_{\rm FC}$ is determined in a complex way by pinning, as discussed elsewhere.[5] Because this value is, in general, different from M_{ZFC}, the internal fields of the two experiments are different. For

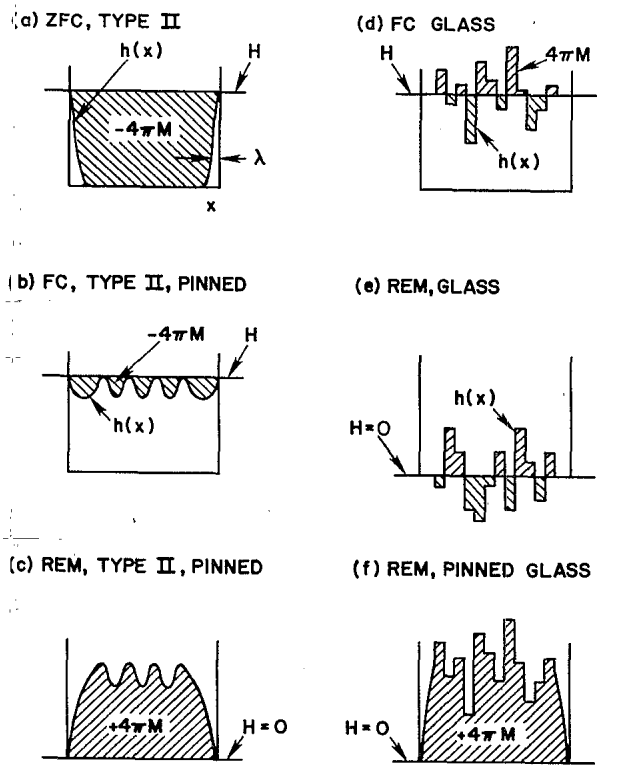

FIG. 7. Schematic contours of applied field H and local magnetic induction $h(x)$ across a superconducting sample. The behavior of a conventional pinned type-II superconductor is illustrated in (a)–(c), while the behavior of a superconductive glass (Refs. 10 and 11) is illustrated in (d) and (e). In (a) zero-field cooling with $H<H_{c1}$ gives flux penetration only within a London penetration depth at the surface. The shaded area with downward sloping lines corresponds to a negative magnetization $-4\pi M$. In (b) field cooling leads to flux trapping and a significantly reduced negative magnetization. In (c) the remanent moment is positive and is indicated by the shaded area with upward sloping lines. In (d) the random polarities of local currents in the superconducting glass give moment variations on a scale set by the structure of Josephson junctions in the material; their amplitude averages to zero for sufficiently large field. In (e) the net remanent moment of the superconductive glass is zero even though the local moments may be randomly positive or negative. Finally, in (f) the hypothetical "pinned" superconductive glass preserves the configuration of (d) within the material and gives a positive net magnetization.

field cooling the internal field is $H_a-4\pi NM_{\rm FC}$, so that

$$B_{\rm FC}=H_a-4\pi NM_{\rm FC}+4\pi M_{\rm FC}. \tag{5}$$

Finally, we consider the remanent moment when the field is turned off. If we assume all the flux in the bulk of the sample remains pinned, as illustrated in Figs. 7(b) and 7(c), B remains by definition $B_{\rm FC}$. To determine the remanent moment, we note that it will generate its own demagnetizing fields $-4\pi NM_{\rm rem}$. Since the applied field is now zero, we have

$$B_{\rm FC}=4\pi(1-N)M_{\rm rem}. \tag{6}$$

Eliminating $B_{\rm FC}$ and solving Eqs. (5) and (6) for $M_{\rm rem}$,

and substituting Eq. (4), we recover Eq. (1) identically.

We conclude that the raw comparisons in Figs. 3–6, which verify Eq. (1), support the flux-pinning picture. A prediction of the unusual field dependence of M_{FC} in this picture has been given earlier[5] and will be extended to include demagnetizing effects in later work.

IV. REMANENT MOMENT IN THE SUPERCONDUCTIVE GLASS MODEL

A. Superconductive glass model: Introduction

The superconductive glass model[9–11] offers a very different interpretation of the reduction in field-cooled moment from its ideal Meissner ratio of 100%. In the following sections we develop the expected behavior of the low-temperature field-cooled, zero-field-cooled, and remanent moments in this model. We extend the model beyond earlier treatments so as to compare as well as possible to experiment, but as will be seen, even with these extensions there remain significant problems in the comparison to crystal data. Finally, then, this analysis points back to flux pinning as the most coherent interpretation for the magnetic properties of crystals. Nevertheless, many of the ideas in this section may still be relevant to ceramics, where a glassy model is physically more plausible.

We start with a brief review of the model,[10] which consists of a system of superconducting grains, usually taken to be small compared to the London penetration depth, and described by a complex order parameter with phase ϕ_i for the ith grain. The grains i and j are coupled by a coupling energy J_{ij}, with the Hamiltonian

$$\mathcal{H} = -\sum_{i,j} J_{ij}\cos(\phi_i - \phi_j - A_{ij}) , \tag{7}$$

where the phase factor or "gauge field" A_{ij} is determined by the vector potential $\mathbf{A}$ according to

$$A_{ij} = (2\pi/\Phi_0)\int_i^j \mathbf{A}\cdot d\mathbf{l} , \tag{8}$$

and where Φ_0 is the flux quantum $hc/2e$.

Equation (7) leads[10] to a Josephson-like current between grains i and j

$$I_{ij} = (2eJ_{ij}/h)\sin(\phi_i - \phi_j - A_{ij}) , \tag{9}$$

and a cluster moment

$$\mu = (1/2c)\sum_{i,j} \mathbf{X}_{ij}\times I_{ij}\mathbf{x}_{ij} , \tag{10}$$

where $\mathbf{X}_{ij}$ is the vector joining the origin to the midpoint between grains i and j and where $\mathbf{x}_{ij}$ is the vector distance from grain i to grain j.

Insight into the predictions of this model can be obtained by considering a single loop of N grains enclosing an area S, connected by equal coupling energies J, as discussed by Ebner and Stroud.[10] The gauge-field phase factors A_{ij} between two grains, given by $2\pi BS/N\Phi_0$, determine the current I according to Eq. (9) and the moment IS/c from Eq. (10). There are multiple states for the system, corresponding to N different choices of the phase difference $\phi_{ij} = 2\pi m/N$ between two neighboring grains, where $0 < m \leq N$ is an integer. Whenever B is near a multiple of ϕ_0/S, it is favorable for the system to adjust the phase difference ϕ_{ij} to compensate for A_{ij}. Lowest energy for this system (see Fig. 1 of Ref. 10) thus corresponds to the zigzag current pattern illustrated by the solid lines in Fig. 8 for the case of a loop with $N = 6$ elements, and the moment is proportional to this current. Between these states, however, are energy barriers; so low-temperature field excursions cause the current to follow the full sine waves in Fig. 8 into the metastable dashed regions.

If the loop sizes or shapes are random, the resulting random gauge-field phase factors A_{ij} give rise to random currents and hence random moments. Figure 8 shows that if the field B is of order Φ_0/S with S an average loop size of a distribution spread over a range S, the currents can be of either sign, i.e., clockwise or counterclockwise around the loop, and the corresponding moments can be either positive or negative. In fact, simulations of more complex systems show[11] that above some lower critical field H_{nl}, which is probably determined by the size of the array,[4] and which is in any case considerably smaller than Φ_0/S, the magnitude of the net array moment actually

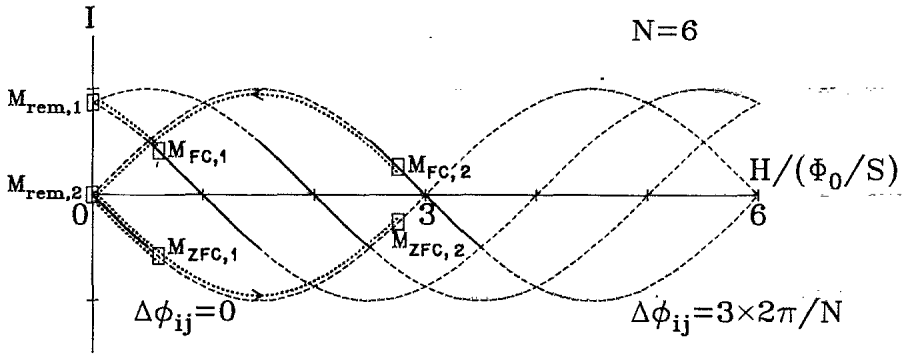

FIG. 8. Current for the first four flux states of a six-member Ebner-Stroud (Ref. 10) loop. Two cases for determining the FC, ZFC, and REM moments are illustrated for $H/(\Phi_0/S)$ equal to 0.6 and 2.75. The first case, labeled 1, corresponds to H close to zero, so that M_{rem} closely approximates $M_{FC} - M_{ZFC}$. The second case, labeled 2, corresponds to the limit for true glassy behavior in which M_{rem} has no simple relation to $M_{FC} - M_{ZFC}$.

drops with increasing field because of increasing local moment reversal. The moment reaches essentially zero for applied fields of order Φ_0/S. At this point there are equal numbers of local moments pointing up and down, and the system can be termed completely frustrated. This provides a possible interpretation for the experimental field-dependent Meissner fractions shown in Figs. 3–6.

Such reversed polarity moments are physically measurable, and we propose that their presence should be considered as a defining experimental test of the superconductive glass. This is because the random gauge fields giving random current polarities are a central feature of the theory. If this feature is absent and all the moments point in the same direction, then the system can be equally well treated by a conventional critical state and flux-pinning model for an Abriksov vortex lattice.

For example, flux line decoration techniques[20] should permit the direct observation of the reverse polarity moments. The density of the lines would differ from that expected for conventional flux pinning, since in the glass it is determined by the structural arrangement of Josephson junctions, whereas in the Abrikosov lattice it scales as H/Φ_0. Magnetooptic decoration techniques might directly detect the sense of the flux lines through the sign of the magnetooptic Kerr rotation.[21] Yet another method is to measure the difference between the remanent moment and $M_{FC}-M_{ZFC}$, as will be discussed in the following sections.

B. History-dependent moments in the superconductive glass model

Next let us consider the behavior of field-cooled, zero-field-cooled, and remanent moments in a superconductive glass model without screening (i.e., $B=H$), appropriate for the limit of small coupling J. The important effect of screening will be discussed in the next section.

Let us first consider the effect of a low field ($H \ll \Phi_0/S$) on the single loop described above and in Fig. 8. Zero field cooling corresponds to starting at $H=0$ in the lowest energy state and moving along the initially solid contour down and to the right in Fig. 8. This generates a negative or diamagnetic moment called $M_{ZFC,1}$ in the figure, although in this model without screening, the moment is usually small compared to the conventional Meissner screening $M/H=-1/4\pi$. Field cooling follows the same contour unless the field is slightly larger than $\Phi_0/2NS$, in which case the system hops to the next solid segment, as shown by $M_{FC,1}$ for a field $H/(\Phi_0/S)=0.6$ in Fig. 8. The remanent moment is determined by following this contour to zero field, giving a net positive value called $M_{rem,1}$ in the figure. In the limit of large N, the remanent moment equals the difference of the field-cooled and zero-field-cooled moments at the same field because the first two contours are parallel to each other.

However, at higher fields, for instance at $H/(\Phi_0/S)=2.75$, Fig. 8 shows that the zero-field-cooled moment $M_{ZFC,2}$ corresponds to about -0.25, while the field-cooled moment $M_{FC,2}$ corresponds to $+0.25$ and the remanent moment $M_{rem,2}$ to 0. Clearly, because of the nonlinearity, there is no necessary connection between the remanent moment and $M_{FC}-M_{ZFC}$.

This argument may now be extended to a more complex system with an uncoupled distribution of loop sizes S randomly distributed over some interval of order S. For fields of the order of the average Φ_0/S, there will then be a distribution of values of $H/(\Phi_0/S)$ spreading over a full wavelength of the sine-wave contour in Fig. 8, and the distribution of moments of individual loops will take on all possible values, both positive and negative, such that the average moment will approach zero in a large system. A schematic distribution of the local induction field $h(x)$ is shown in Fig. 7(d), where the positive and negative spikes around the average level of the applied field H represent the random moments of the different loops.

When the applied field is reduced to zero without any hopping from contour to contour, the average remanent moment must also be zero because the starting points and distances traveled along the B axis in Fig. 8 are all random. It is reasonable to suppose that a more complex model of coupled loops would behave similarly, although this needs to be verified by simulation. It is important to note that in this model without screening the field H is an independent variable; so there is no tendency to trapping or pinning of flux in the usual sense. The final distribution of the local induction field at $H=0$ will look like Fig. 7(e), where on average the random distribution of local-field variations is similar to that of Fig. 7(d), but it is translated downwards by an amount H and the precise moment values at any given location are randomly different.

Thus, in a model with no screening, zero field cooling cannot lead to any exclusion of field. The zero-field-cooled state will resemble that of Fig. 7(d), though again with a different precise contour of $h(x)$. Thus, the net zero-field-cooled moment will also be zero. Although $M_{rem}=M_{FC}-M_{ZFC}=0$, these predictions obviously bear little relation to the experimental results where M_{ZFC} and M_{rem} are both substantial. A first step to correct these difficulties and to provide a mechanism for the complete flux exclusion observed in zero field cooling is to introduce screening into the superconductive glass model.

C. Superconductive glass model with screening

As a first step towards introducing screening[22] in the superconducting glass model, let us imagine a system of loops of area $S=a^2$ with centers on a simple cubic grid of lattice parameter a. Let us assume the system has an needle shape, so that overall demagnetizing factors are negligible. In the low-field limit $B \ll \Phi_0/a^2$, we may expand the sine in Eq. (9) and calculate a magnetization or moment per unit volume μ/a^3 (in cgs units) by combining Eqs. (8)–(10):

$$4\pi M=-(8\pi^2 Ja/N\Phi_0^2)B\equiv-\eta B\,, \tag{11}$$

where as usual $B=H+4\pi M$ and where η is a positive dimensionless parameter which measures the strength of the screening. Solving for $4\pi M$, one has

$$4\pi M=-\eta H/(1+\eta)\,. \tag{12}$$

Thus if η is large the system is fully screened ($B \rightarrow 0$), whereas if η is small $4\pi M$ is inadequate to compensate for H.

Let us estimate η, assuming that the coupling energy J can be related to the critical current density J_c by $J_c = 2eJ/ha^2$. This gives

$$\eta = 8\pi^2 J_c a^3/c\Phi_0 . \tag{13}$$

There is, of course, uncertainty in equating the macroscopically measured current density with this hypothetical microscopic parameter J_c because frustration might make it impossible for the sample to simultaneously support a current density J_c everywhere. In this sense the estimates for η are a lower limit. Typical parameters for Y-Ba-Cu-O ceramics and crystals are given in Table II. A presumed grain size for the hypothetical glassy crystal is taken to be a twin spacing of order 100 nm, following on the suggestion[23] that twin planes might be acting as effective Josephson junctions. The estimates in Table II show that typical ceramics fall in the strongly screened limit while crystals may be only weakly screened.

Going beyond the weak-field limit, we expect onset of nonlinearities in M vs H or B, just as discussed in the predeeding section. Let us define this to occur when B becomes a fraction f of Φ_0/a^2, which, according to Eq. (12), implies

$$H_{\rm nl}/(\Phi_0/a^2) = f(\eta+1) . \tag{14}$$

The fraction f has been calculated in several simulations[10,11] and is of order 0.1 to 0.01, although as discussed elsewhere[4] these results most likely depend on the size of the array used in the simulations and will drop as the array becomes larger. We will use the value $f = 0.01$ below.

This "nonlinearity" critical field can be compared to a number of other critical fields derived by considering screening without nonlinear effects. In addition to the possibility of screening by local internal currents, there is the possibility of screening by a current running through junctions adjoining the surface of the sample. This situation, recently treated by Clem,[24] is controlled by a Josephson penetration depth between two adjacent grains having a London penetration depth λ assumed much larger than the Josephson barrier thickness. This penetration depth can be expressed, using our dimensionless screening parameter η, as

$$\lambda_{J,g}/a = (a/2\lambda\eta)^{1/2} . \tag{15}$$

For the derivation to be consistent, $\lambda_{J,g}$ must be less than the grain size a; otherwise the problem shifts to the intergranular limit discussed below.

From the Maxwell equation $dh/dx = 4\pi J/c$, one derives a critical field beyond which the junction is no longer able to carry enough screening current to fully shield the sample:

$$H_{{\rm crit},g}/(\Phi_0/a^2) = (\eta a/2\lambda)^{1/2}/2\pi . \tag{16}$$

Here, the subscripts "g" refer to the "grain" and the fact that the results depend on the intragranular London penetration depth λ.

Estimates in Table II show that for both ceramics and the hypothetical glassy crystals, the condition $\lambda_{J,g} \leq a$ is approximately satisfied, although clearly somewhat lower values of J_c would have given the opposite result. We recall, however, that the local J_c is likely to be larger than the measured bulk J_c as discussed earlier. Comparing now $H_{\rm nl}$ with $H_{{\rm crit},g}$, we find that for $f = 0.01$ and for the Table II parameters, the latter is larger.

These estimates show that surface currents can shield the interior even at fields which would induce nonlinearities (local moment reversals) in the granular superconductor. Thus it provides a way to reconcile the essentially complete flux exclusion generally observed in zero-field-cooled measurements with glassy suppression of moment in field-cooled measurements at one and the same applied field. In other words, zero field cooling in fields below $H_{{\rm crit},g}$ will give full flux exclusion. For the Table II parameters, this corresponds to 0.2 Oe in the granular material and 200 Oe in the hypothetical glassy crystal, well within the range we have studied. On the other hand, field cooling should give near complete flux expulsion (because of the large η) only below $H_{\rm nl} = 0.16$ Oe for the ceramic and partial flux expulsion below 36 Oe for the crystal, with the flux expulsion dropping towards zero at 0.2 and 2000 Oe, respectively. While these predictions qualitatively resemble some of the FC and ZFC data, we have not found a way to adjust the input parameters so as to match the data quantitatively.

The remanent moment poses further problems. In the range of fields where flux exclusion is largely complete but flux expulsion is dominated by glassy effects, we can make the following rough model. We assume conventional flux pinning with pinned magnetization M_p in a volume fraction f_p of the sample, for instance within the grains. The remainder of the sample $f_g = 1 - f_p$ can be assumed to consist of glassy regions where the magnetization is totally neutralized by random orientation of the local moments. During field cooling only the "nonglassy" regions develop screening currents, and so the field-cooled magnetization $M_{\rm FC}$ is just $f_p(M_p - H/4\pi)$. The remanent magnetization $M_{\rm rem}$ is $f_p M_p$, while the zero-field-cooled magnetization is, according to our above discussion, the complete exclusion $-H/4\pi$. Combining these quantities, we find

$$4\pi(M_{\rm rem} - M_{\rm FC} + M_{\rm ZFC})/H = f_g . \tag{17}$$

TABLE II. Typical parameters for Y-Ba-Cu-O ceramics and crystals (see definitions in text).

	Ceramic	Crystal
J_c (A/cm^2, $T=0$)	2×10^3	2×10^7
a (cm)	10^{-3}	10^{-5}
λ (cm)	10^{-5}	10^{-5}
$\eta = 8\pi^2 J_c a^3/c\Phi_0$	80	0.8
$a/2\lambda$	50	0.5
Φ_0/a^2 (Oe)	0.2	2000
$H_{\rm nl}$ (Oe, $f=0.01$)	0.162	36
$\lambda_{J,g}/a = (a/2\lambda\eta)^{1/2}$	0.79	0.79
$H_{{\rm crit},g}$ (Oe)	2	201
$\lambda_{J,i}/a = \eta^{-1/2}$	0.11	1.1
$H_{{\rm crit},i}$ (Oe)	0.2	284

This suggests that the difference between $M_{\rm rem}$ and $M_{\rm FC}-M_{\rm ZFC}$ is a measure of the "glassy" volume fraction f_g. Experiment shows that this fraction is zero within experimental error in all the systems, including, surprisingly, the ceramic samples studied so far (see Fig. 3 and Ref. 3).

We can make a simple estimate of f_g which shows the sensitivity of this test. According to Fig. 13 of Ref. 11, simulations show that at $H/(\Phi_0/S)=0.03$, M has dropped 10% from its peak value because of glassy polarity reversals. The value 0.03 corresponds to the ratio of our largest measurement field of 60 Oe to $\Phi_0/S=2000$ Oe (see Table I). Since the glassy fraction does not contribute to the remanent moment, we would expect f_g in Eq. (17) to be of the order of 10%, whereas our experiment shows it to be within experimental error (1%) of zero.

Nevertheless, one should not be too hasty to reject the glassy model. We consider several other possibilities for reconciling the model with the data. One is to consider that the condition $\lambda_{J,g}<a$ for the Josephson penetration model is not satisfied and that the field penetration spreads across many grains. This limit was first treated in the context of high-temperature superconductors by Raboutou *et al.*,[25] who derived the effective intergranular Josephson penetration depth, which in our units can be simply expressed:

$$\lambda_{J,i}/a=\eta^{-1/2}. \tag{18}$$

The corresponding critical field is

$$H_{{\rm crit},i}/(\Phi_0/a^2)=(\eta/2)^{1/2}/2\pi. \tag{19}$$

For the Table II parameters, the condition $\lambda_{J,i}>a$ is not at all satisfied for ceramic material but is marginally satisfied for crystals, particularly if J_c is low. $H_{{\rm crit},i}$ works out to be 284 Oe for the crystal. In principle, this could extend the range of full flux exclusion to higher fields ($H_{{\rm crit},i}>H_{{\rm crit},g}$), but the same problem with the remanent moment arises as in the earlier treatment of $H_{{\rm crit},g}$, namely that the remanent moment should measure the glassy fraction, and experiment shows it to be essentially zero.

Above these critical fields, there is nothing in the naive model (i.e., ignoring flux pinning; see below) to prevent full penetration of the applied field, which will be only partly shielded by the frustrated magnetization it induces in the sample. Thus one would expect significant deviations from full ZFC flux exclusion at fields in the range of 0.2 or 284 Oe for ceramics and crystals, respectively (see Table II). This is again largely in contradiction with the crystal experiments, where the lower critical fields are observed to be significantly larger, at least for H$\|$c.[26]

Because of the glassy effects, one cannot assume a coherent Josephson-like penetration once the field exceeds $H_{\rm nl}$. Glassy regions reduce screening and increase flux penetration. They do this increasingly as the glassy fraction increases above $H_{\rm nl}$ and approaches 1 near Φ_0/a^2. At this latter field the effective penetration depth should diverge. It would be an interesting problem, though beyond the scope of this paper, to simulate this effect numerically in a random lattice of Josephson junctions.

Finally, we consider yet another possible avenue for the glassy model to explain the experimental findings. Throughout the discussion so far, we have assumed, following the original models, that the internal field is an independent variable, determining the magnetization but not being affected by it. In effect, this amounts to ignoring the possibility of flux pinning. Thus, as illustrated in Figs. 7(d) and 7(e), when applied field is turned off, it has been assumed that the moments are modulated but that the average level of $h(x)$, corresponding to the applied field H, simply shifts to zero. From a macroscopic point of view this is a reasonable assumption since the average energy of a fully random system is the same in the zero-field remanent state as in a field of order Φ_0/a^2.

However, it is possible that the *local* disordered dipolar fields modulate the internal field in such a way that local barriers develop against flux change. This could lead to pinning of the overall flux distribution $h(x)$. A simulation of such pinning in random Josephson arrays would be an interesting problem for the future. Let us simply assume here that it is very strong. In this case reducing the applied field to zero would cause a change from the configuration of Fig. 7(d) to that of Fig. 7(f). The same pinning would prevent penetration of flux in a zero-field-cooling experiment. In this case it is obvious that the condition $M_{\rm rem}=M_{\rm FC}-M_{\rm ZFC}$ would be satisfied.

This hypothesis resolves some basic problems in comparing glassy theory to experiment. However, the glassy model now becomes difficult to distinguish from more conventional flux pinning, at least from a macroscopic point of view. But the microscopic parameters of the flux pinning picture would now have a different interpretation, the activation barriers and jump distances being determined by the random Josephson array rather than by conventional defect pinning.

The two pictures can be distinguished microscopically, however, because, as mentioned earlier, the distribution of moments in the superconductive glass picture bears no necessary relation to a set of well-defined Abriksov flux lines with flux quantum $\Phi_0=hc/2e$. Magnetic decoration techniques are sensitive to the variations in $h(x)$, and therefore the density of decoration centers is a good indication of the nature of the moment distribution. Such experiments, performed on crystals,[20] have shown a flux lattice at sufficiently low temperatures, with quanta Φ_0 in a field range where, based on Table II parameters, a significant glassy contribution should occur. This observation would appear to exclude the superconductive glass interpretation, even with the pinning hypothesis, at least in the low-temperature regime.

V. CONCLUSIONS

In summary these considerations, coupled with our observations of remanent moment and the earlier flux decoration experiments, argue against the superconductive glass interpretation for crystals, at least in the low-temperature, low-field range. This point of view is supported by the earlier[5] semiquantitative interpretation of the field dependence of the field-cooled moment and also by the explanation of the irreversibility line,[12] using a more conventional flux-pinning picture.

However, for Y-Ba-Cu-O ceramics, it is now an estab-

lished fact[27] that the boundaries between grains act like Josephson elements; so it would seem that the criteria for the superconducting glass model are all present. In this case it would be more difficult to do a decoration experiment: The field range is significantly less (see Table II) and sample inhomogeneity makes interpretation of the images more difficult.

There are two possibilities to explain the good agreement between $M_{\rm rem}$ and $M_{\rm FC}-M_{\rm ZFC}$ in ceramics. One is to invoke strong glassy flux pinning; this hypothesis still needs to be investigated in theoretical simulations to demonstrate its plausibility. The other is to suppose that the large grains of the ceramic dominate the macroscopic magnetic behavior so that the glassy contributions, while present, are simply smaller than present experimental error. This is plausible because the intergranular regions, where glassy contributions should originate, represent only a small fraction of the total volume of high-density ceramics. A possible approach to this problem would be to study much finer grain ceramics, a topic of considerable interest in any case for synthesis of possibly higher current density material.

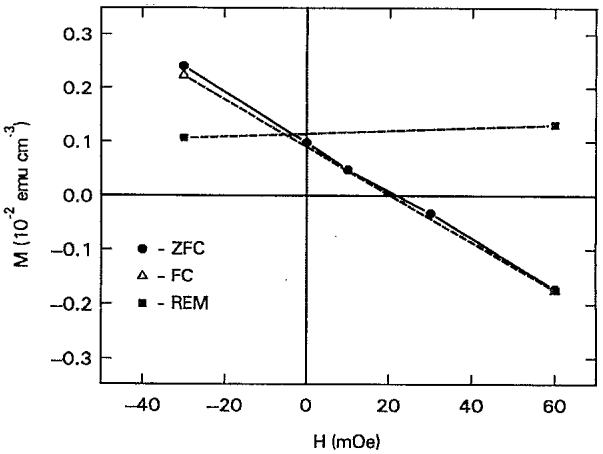

FIG. 9. Field-cooled, zero-field-cooled, and remanent moments of another thin crystal similar to that in Fig. 6, in a range of positive and negative fields around zero. The results show the offset due to a background ferromagnetic impurity when the sample signal is very small.

ACKNOWLEDGMENTS

The authors acknowledge many people for valuable discussions: K. A. Müller, J. R. Clem, J. Evetts, D. K. Finnemore, P. H. Kes, J. A. Mydosh, T. K. Worthington, T. R. McGuire, T. Schneider, and I. Morgenstern. They thank E. Engler, V. Lee, C. Tsuei, and T. R. Dinger for ongoing interactions on a variety of superconducting materials.

APPENDIX

We describe here some details of our experimental results and analysis which become important at low fields and for small sample sizes where signals are very small. An example of zero-field-cooled, field-cooled, and remanent measurements on the ultrathin crystal are shown in Fig. 9 for fields of ± 50 mOe. The data, which normally would be expected to intersect zero, show an offset which can be interpreted as a background signal. In this region the traces of signal versus sample position in the magnetometer show distortion, suggesting the presence of tiny ferromagnetic impurities on the sample holder. These signals vary in size in different measurements, and even with reasonable precautions about cleanliness, we have not been able to routinely eliminate these effects.

Without taking this effect into account, the data of Fig. 9 might mistakenly be taken to indicate a large enhancement of M/H near zero field. They could also mistakenly be taken to indicate a failure of the rule $M_{\rm rem}=M_{\rm FC}-M_{\rm ZFC}$. However, we interpret the intersection of these curves with the vertical axis in Fig. 9 as a background ferromagnetic signal which we subtract off from all the data. Then we see that the $M_{\rm rem}$ rule is preserved and M/H is well behaved near zero field. This correction has been made in Figs. 3–6.

*Permanent address: Department of Physics, Bar-Ilan University, Ramat-Gan, Israel.

[1]H. Maletta, A. P. Malozemoff, D. C. Cronemeyer, C. C. Tsuei, R. L. Geene, J. G. Bednorz, and K. A. Müller, Solid State Commun. **62**, 323 (1987).

[2]T. R. McGuire, T. R. Dinger, P. Freitas, W. J. Gallagher, T. S. Plaskett, R. L. Sandstrom, and T. M. Shaw, Phys. Rev. B **36**, 4032 (1987); T. R. McGuire, F. Holtzberg, D. L. Kaiser, T. M. Shaw, and S. Shinde, J. Appl. Phys. (to be published).

[3]D. C. Cronemeyer, A. P. Malozemoff, and T. R. McGuire, in *High Temperature Superconductors,* edited by M. B. Brodsky, R. C. Dynes, K. Kitazawa, and H. L. Tuller (Materials Research Society, Pittsburgh, PA, 1988), Vol. 99, p. 837.

[4]L. Krusin-Elbaum, A. P. Malozemoff, and Y. Yeshurun, in *High Temperature Superconductors,* edited by M. B. Brodsky, R. C. Dynes, K. Kitazawa, and H. L. Tuller (Materials Research Society, Pittsburgh, PA, 1988), Vol. 99, p. 221. The temperature calibration of these measurements was in error; T_c should have been given as 89 K.

[5]L. Krusin-Elbaum, A. P. Malozemoff, Y. Yeshurun, D. C. Cronemeyer, and F. Holtzberg, in *Proceedings of the International Conference on High Temperature Superconductors and Materials and Mechanisms of Superconductivity, Interlaken, Switzerland, 1988,* edited by J. Müller and J. L. Olsen [Physica C **153–155**, 1469 (1988)].

[6]P. W. Anderson, Phys. Rev. Lett. 9, 309 (1962); Y. B. Kim, Rev. Mod. Phys. **36**, 39 (1964).

[7]A. M. Campbell and J. E. Evetts, Adv. Phys. **21**, 199 (1972).

[8]M. Tinkham, *Introduction to Superconductivity* (McGraw-Hill, New York, 1975).

[9]K. A. Müller, M. Takashige, and J. G. Bednorz, Phys. Rev. Lett. **58**, 1143 (1987).

[10]C. Ebner and D. Stroud, Phys. Rev. B **31**, 165 (1987).

[11]I. Morgenstern, K. A. Müller, and J. G. Bednorz, Z. Phys. B **69**, 33 (1987); see also, J. V. Jose (unpublished).

[12]Y. Yeshurun and A. P. Malozemoff, Phys. Rev. Lett. **60**, 2202 (1988).

[13]P. Norling, P. Svedlindh, P. Nordblad, L. Lundgren, and P.

Przyslupsky, in Ref. 5, p. 314.
[14]M. Tuominen, A. M. Goldman, and M. L. Mecartney, Phys. Rev. B **37**, 548 (1988); in Ref. 5, p. 324.
[15]C. Rossel and P. Chaudhari, in Ref. 5, p. 306.
[16]M. E. McHenry, M. Foldeaki, J. McKittrick, R. C. O'Handley, and G. Kalonji, in Ref 5, p. 310.
[17]W. J. Gallagher, R. L. Sandstrom, T. Dinger, T. M. Sahw, and D. Chance, Solid State Commun. **63**, 147 (1987).
[18]E. Engler and V. Lee (private communication). The high-density Y-Ba-Cu-O ceramic was prepared by a near-melt processing, heating previously sintered material (at 900 °C for 24 h) at 1010 °C for 36 h.
[19]F. Holtzberg, D. L. Kaiser, B. A. Scott, T. R. McGuire, T. N. Jackson, A. Kleinsasser, and S. Toner, in *Chemistry of High Temperature Superconductors,* edited by D. L. Nelson, M. S. Wittingham, and T. F. George ACS Symposium Series, Vol. 351 (American Chemical Society, Washington, DC, 1987), p. 79.
[20]P. L. Gammel, D. J. Bishop, G. J. Dolan, J. R. Kwo, C. A. Murray, L. F. Schneeneyer, and J. V. Waszczak, Phys. Rev. Lett. **59**, 2592 (1987).
[21]R. Gambino (private communication).
[22]T. Schneider (unpublished).
[23]G. Deutscher and K. A. Müller, Phys. Rev. Lett. **59**, 1745 (1987).
[24]J. R. Clem, in Ref. 5, p. 50.
[25]A. Raboutou, P. Peyral, J. Rosenblatt, C. Lebeau, O. Pena, A. Perrin, C. Perrin, and M. Sergent, Europhys. Lett. (to be published).
[26]Y. Yeshurun, A. P. Malozemoff, F. Holtzberg, and T. R. Dinger (unpublished).
[27]P. Chaudhari, J. Mannhart, D. Dimos, C. C. Tsuei, J. Chi, M. Oprysko, and M. Scheuermann, Phys. Rev. Lett. **60**, 1653 (1988).